

EVALUATING THE OFF POSITION FOR E-PERM SENSORS CONFIGURED WITH S CHAMBERS IN A HIGH RADON CAVE ENVIRONMENT

Lawrence E. Welch*, Abigail R. Van Blarcom, Christopher P. Andreou,
Mark D. Jones, and Michael J. Lace

Knox College
Galesburg, Illinois, USA

lwelch@knox.edu

Abstract

E-PERM (Electret Passive Environmental Radon Monitor) sensors have been demonstrated to proficiently and accurately measure radon concentrations in humid and particulate-rich cave environments. By selecting the electret style, the chamber type, and the experiment duration, radon levels can be evaluated over a wide range of concentrations with these sensors. Prior studies have demonstrated that an active experiment can be terminated by closing the chamber and transporting an off-position E-PERM out of the cave while the electret is still installed without alteration of the experimental data, but this transport process only spanned a short period of time. The current study evaluates whether the E-PERM will continue to register signal if left in the off position for an extended time period within a radon-rich cave environment.

The authors have received partial funding from Knox College to support the research leading to this publication, including allocations from the Billy Geer Fund, the Andrew W. Mellon Foundation, the Committee on Faculty Research, and the Paul K. and Evalyn Elizabeth Cook Richter Trusts.

Introduction

E-PERM (Electret Passive Environmental Radon Monitor) units are a type of EIC (Electret Ion Chamber) sensor that have been commonly used to measure radon levels in a variety of sampling locales (Kotrappa, 1988; Kotrappa, 1990; Fjeld, 1994). Each E-PERM consists of a chamber and an electret, with the electret installed by screwing it into the bottom of the chamber. Chambers are available in differing sizes, which offer differing degrees of sensitivity to radon; the larger the chamber volume, the greater the signal produced for a given radon concentration. Likewise, different types of electrets with varying sensitivities can be mated with the chamber, providing another tool to customize the response of the sensor.

The S chamber is a commonly-used E-PERM chamber that has been described and depicted graphically in Stacks (Stacks, 2015). This chamber has an internal volume of 210 ml. Alpha decays within the chamber can ionize proximate air molecules, with the electrons subsequently being collected by a positively-charged electret that is installed in the chamber. The S chamber has an on/off switch. To turn the chamber on, the chamber cap is unscrewed counterclockwise and the cap pops up via a spring-loaded mechanism, opening the ingress pathway. This permits passive entry, but the pathway includes a filter which precludes all except gases from entering the chamber. When the cap is pushed down and tightened by screwing it clockwise, the chamber locks into the off position. In this position, open access to the input filter is blocked. Inside the chamber when it is turned off, a plunger drops down to cover the electret, blocking access to the positively-charged electret surface for most of the chamber volume. Only the tiny air volume trapped between the plunger and the electret surface will feel the influence of the positive charge that resides on the surface of the electret. The RT chamber (also known as the Radon-Thoron S Chamber) is made from an S chamber and maintains the same 210-ml volume. It has a series of holes cut in the side of the thermoplastic shell of the chamber, which are then covered with a layer of 0.13 mm thick Type 14 Tyvek (Kotrappa, 2010), which radon easily passes through with an estimated delay time of only 8 seconds under passive conditions (Kotrappa, 2014). This provides quicker gaseous entry into the chamber than via the traditional pathway through the filter in the sensor neck, producing a more-responsive sensor that can measure most of the short-lived (half-life 55.6 seconds, Rumble, 2018) ^{220}Rn present in the air in addition to ^{222}Rn . The standard S chamber only detects 3% of the ^{220}Rn due to the short half-life coupled with the requirement for passive gas entry, as most atoms of this radionuclide cannot traverse the inlet filter and enter the chamber before they decay (Stacks, 2015; Welch, 2022).

This research group has used E-PERM sensors extensively to measure radon concentrations in caves (Welch, 2016, 2017, 2019, 2021, 2022, 2024). The E-PERMs have proven robust for operating in these environments, which typically feature high humidity and high airborne particulate levels, while often necessitating significant transport to reach the desired sampling sites. One concern mentioned in past reports has been how to transport the sensors out of the caves (Welch, 2016, 2023). After a trial is complete, the chamber is closed and the electret is typically screwed out of the chamber and sealed with a thermoplastic cap. However, if this is done within the cave environment, the active surface of the electret is exposed to the harsh cave environment, and an experimentalist risks water droplets and solid particulates impacting the

electret during the changeover, which can cause the electret voltage to change. The earlier studies examined shutting off the chamber and then transporting the entire sensor out of the cave without removing the electret. The electret could then be removed and capped in a blank environment with a much lower risk of liquid or solids coming in contact with the sensitive surface of the electret. These prior studies showed that there was no significant voltage shift in removing the E-PERMs from the cave with the electrets still installed, so this procedure was adopted as standard for in-cave measurements. However, it should be noted that the cave removal process in the cited studies was completed in tens of minutes as opposed to tens of hours, and some subtle cues from the studies suggested that if the removal process entailed the installed electrets spending many hours in a high-radon environment while in the off-position chamber, that the results might have been different.

In this study, a series of probes were made to delve more deeply into this phenomenon, whereby E-PERMs were placed in Coldwater Cave with its high radon concentration (Welch, 2021) for an extended period of time with the electret installed in the chamber while it was kept in the off position, to evaluate whether that would cause a significant voltage change on the part of the electret.

Materials and Methods

Equipment

Integrated average radon concentrations were measured with E-PERM EIC sensors, consisting of an electret of the short-term [ST] variety, and a chamber of the S or RT variety, each with a volume of 210 ml, all from Rad Elec Inc. Sets of four to eight E-PERMs were used per trial to improve data precision, and the Grubbs Test at a 90% confidence level was used to evaluate and reject outlying data points in the sets (Grubbs, 1969; Harris, 2017, Welch 2017). Statistical significance was evaluated using a two-sample T-test. Electrets were always installed in the chambers within a blank low-radon environment prior to deploying them in the cave, to ensure the chamber started the trial containing blank air. Electret voltages were measured with a SPER-1E electret voltage reader (Rad Elec). Calculations were done with Radon Report Manager Software Version 3.8.44 from Rad Elec. Background gamma radiation exposure was evaluated with the Model 2 Gamma Ray Dosimeter manipulated with the Model 909B charger from Arrow-Tech.

Temporal measurements of radon concentrations were undertaken using Radon Recon CRM (Continuous Radon Monitor) sensors and Recon Download Tool software v0.9.7 (Rad Elec Inc.). Recon measurements were acquired at 10-minute increments rather than the standard 1-hour increment via spreadsheet manipulation of the raw data file.

In-cave data presented in the Results and Discussion section were collected at Coldwater Cave Station 1. The layout of the cave and a description of the sampling site have been described in a previous paper (Welch, 2021). This sampling site was selected because it featured consistently high radon levels, and, although the radon level does change slowly over time, it remains nearly

constant within the short time frame of the experiments undertaken (Welch, 2021). To minimize the impact of human visitation on the cave atmosphere in Coldwater Cave, the entrance was sealed immediately after human entry and exit and otherwise kept closed throughout the experimental trials. Blank trials were run in a shed disconnected from the cave, essentially filled with outside air. Typical radon concentrations in the blank environment were in the 0-1 pCi/L range.

When the E-PERMs were deployed in a cave, they were placed in Tyvek bags to shelter them from the cave environment. Earlier work demonstrated that the Tyvek bags do not impact the resultant data from the E-PERM (Stieff, 2012; Welch, 2016). E-PERMs for control trials were also deployed in the Tyvek bags.

Trials using lead plates were performed at Station 1 in Coldwater Cave. This location features a wooden platform built over the cave stream. The top platform surface is two to four feet above the cave stream, depending on the weather, and circa 15 feet below the ceiling of the passage. The side walls are circa 10 feet away from the sensors when deployed. A set of six sensors were placed on top of two stacked lead plates that were each 9/64 inch thick. Two curved side pieces of 47/128 inch thick lead were stood up alongside the sensors, making a nearly oval cross-section chamber around the sensors. A top lead plate of 5/32 inch thick lead was balanced on top of the side pieces. The lead chamber was not sealed or airtight, but shielded the E-PERMs in such a manner that any external radiation traveling in a straight line could only strike the sensors if it had gone through the lead plates. The lead shielding did not form a hermetic seal around the E-PERMs, so any ionizing radiation originating from airborne particulates could potentially bypass the shielding.

The Electret Torque Device (ETD) was built using the Knox College Makerspace facility, and is depicted in Figure (1A). The ETD consists of three parts mated together. The first part is a standard 3/8-inch ratchet wrench, which mates to a Quinn 58705 Digital Torque Adapter. The output of the Digital Torque Adapter fits into a 3/8-inch square hole in the middle of head piece printed via a 3D printer out of ASA (acrylo nitrile styrene acrylate) plastic. The circular orange head piece had inset grooves that aligned with the grooves on the thermoplastic outermost surface of the electrets, engaging with them via a friction fit (Figure 1B). The ETD typically was used to tighten electrets into chambers to a value of 1.0 ft-lb.

Mechanical drawings were made using Fusion 360 software by Autodesk.

Polyethylene bags were one-quart seal top models of the Ziploc® brand from S.C. Johnson and Son.

Daren Drums (also known as Darren Drums or Canyon Kegs) were high density polyethylene containers with a wall thickness of 1.1 mm, made by Curtec and distributed by Imlay Canyon Gear. The units used had a total volume of 3.5 liters and had lids that screwed on with an O-ring seal to make them watertight, but not completely airtight.

All spacer trials utilized spacers custom-fabricated using 3D printers in the Knox College Makerspace facility and made from PETG plastic (polyethylene terephthalate glycol). The

optimum spacer style used in the study was comprised of a circular disk of 1-7/8 inches in diameter and 0.04 inches thick. Extending from the bottom of this piece was a concentric cylinder with a diameter of 1-1/4 inches and a thickness of 0.03 inches. Prior to electret installation, the spacer would be placed atop the electret. The wider circular piece would sit suspended on the thermoplastic flanges surrounding the electret active surface, while the narrower piece would fit down inside the flanges, yet not contacting the active surface. The electret-spacer combination would then be threaded into the chamber and tightened with the ETD to 1.0 ft-lb. This spacer reduced the active chamber volume by slightly less than a half. PETG was not an insulator, but it was also less conductive than the thermoplastic body of the chamber.

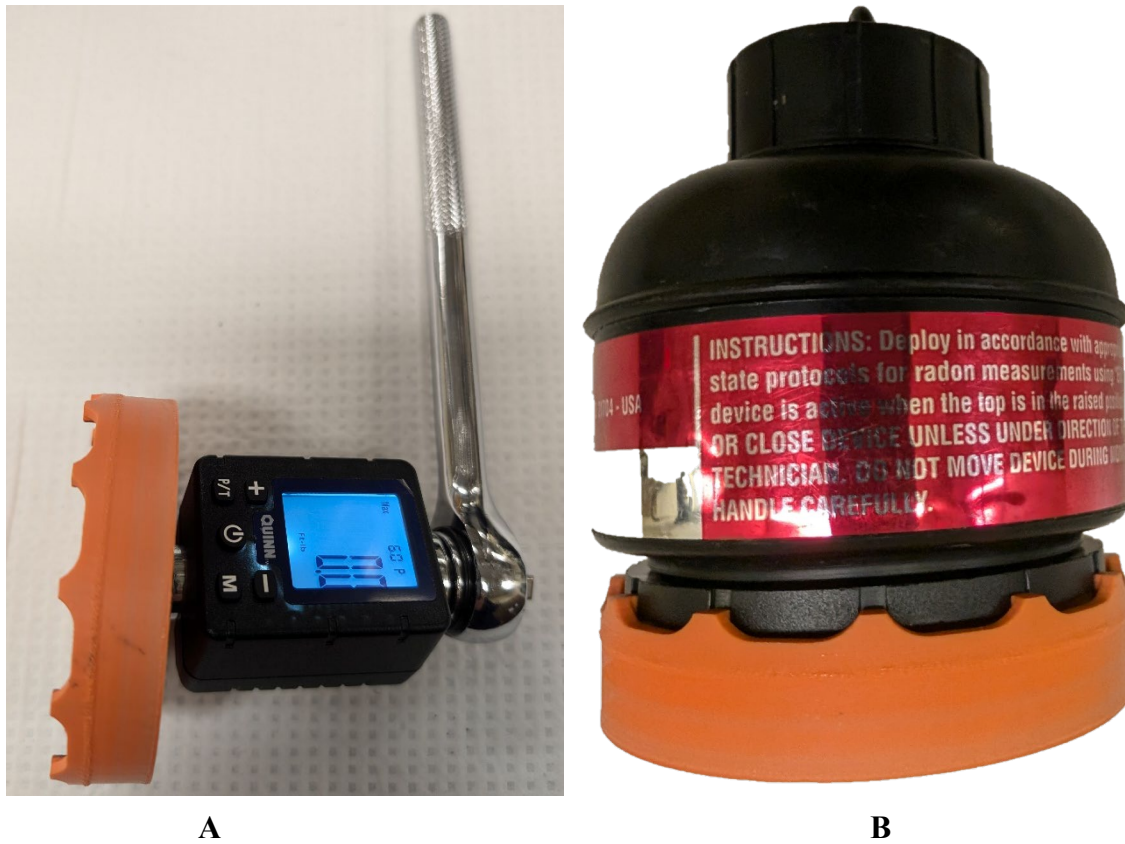


Figure (1): The Electret Torque Device (ETD). Part A shows the three components of the ETD. Part B shows the ETD head piece mating with an installed electret.

A and B Coefficient Determination Methodology

The normal algorithm for calculating radon concentration in pCi/L from the raw voltage readings is given below as Equation (1) (Rad-Elec, 2024).

$$RnC = \left[\left[\frac{(I-F) - (0.066667*D)}{CF*D} \right] - BG * G \right] \quad (1)$$

Where:

RnC = radon concentration in pCi/L

I = initial electret voltage

F = final electret voltage

D = experiment duration in days

CF = calibration factor

BG = background gamma radiation in $\mu\text{R}/\text{Hr}$

G = constant converting BG into pCi/L units, 0.087 used here for S chamber (Rad-Elec, 2024).

The elevation correction terms have been removed from equation (1) for simplicity, since they would not impact the output for all trials undertaken. The calibration factor term can be found as follows in Equation (2).

$$CF = A + B * \ln(\text{MPV}) \quad (2)$$

Where:

MPV = midpoint voltage (average of initial and final voltage)

Equation (1) can be algebraically rearranged to obtain Equation (3).

$$CF = \frac{((I-F) - (0.066667*D))}{(D*(RnC + BG*G))} \quad (3)$$

I, F, and D were derived from the experimental data. BG was typically taken from an average of earlier data at the same location, as the BG sensor would go off-scale if attempting to measure it concurrently with the E-PERM trials in this manuscript. RnC was determined by using a Radon Recon CRM unit running side-by-side with the E-PERM trials. Since I and F are unique to each E-PERM, each sensor would produce an individual calculated CF value from Equation (3). CF values were then paired with the corresponding MPV from each E-PERM, and the data pairs pooled for all the E-PERMs in the set. The CF were then plotted versus the corresponding \ln MPV for each sensor in the pool. From Equation (2), this would be expected to provide a linear plot and the A and B coefficients can then be derived from the slope and intercept of the linear fit. Data from a set of 12 E-PERMs were pooled for each of these plots, with initial voltages spaced widely within a 750 V to 200 V working range. RT chambers were used for all of the trials to determine the A and B coefficients. The RT chamber geometry was exactly the same as for the S chamber, so the coefficients, which are driven by chamber geometry, should be the

same for each. The selection of the RT chambers was based on their additional rapid radon ingress pathway for radon through the Tyvek-covered side pores. The slower ingress seen in the S chambers looked to potentially add another variable, with its inherent uncertainty, to the mix, whereas the rapid ingress for the RT chambers was perceived to minimize variations of this sort.

Results and Discussion

Early trials made it clear that a long duration of time coupled with a high level of radon would be necessary to produce data that would clearly address the issue at hand. Cumulative Radon Exposure (CRE), was a metric created to keep track of these parameters. The CRE value was calculated by multiplying the average radon concentration by the number of hours in duration of the experiment. Early trials with low CRE tallies yielded outcomes that were difficult to interpret, so an experimental goal of greater than 30,000 pCi * Hr / L was pursued as optimal for subsequent trials. It was also necessary to run sets of replicate sensors to improve the precision of the experiment – sets of four to eight were used, with six being the modal value.

Figure (2) shows an experimental outcome featuring simultaneous 71.5-hour duration trials with six replicate sensors in each set, comparing the S and RT chambers in Coldwater Cave at Station 1 along with sets collected in the shed serving as the blank locale. All sensors had electrets installed in a blank environment, and the chamber left in the off position throughout the trial. Radon levels at each of these sites were determined by running Radon Recon CRM sensors side-by-side with the E-PERMs and averaging the temporal data. The shed blank gave a value of 1.1 pCi/L, and the cave 505.8 pCi/L. Using this information, it was determined that the CRE for this trial was 36160 pCi/L – in the desired range. Both chamber types displayed a large and statistically significant difference in ΔV when comparing the cave trial to the blank, with the RT chambers yielding a larger change than that seen with the S chambers. These outcomes suggest that the E-PERM sensors were responding to the radon in the cave air, albeit with a very low sensitivity. If this were true, it would mean that A) radon-rich cave air was getting inside the sensor despite the chamber being off, and B) the space between the electret surface and the plunger that covers the electret in the off position, while small, was large enough that alpha particles from radon were causing air ionization, the electrons from which were being collected by the electret. In other words, the small space between the plunger and electret was acting as a de facto EIC chamber volume, and the sensor was responding as it was designed. The term “active chamber” will be used forthwith to describe this small space between the plunger and the electret in the off position. For comparison, the Inherent Voltage Discharge (IVD) for an ST electret is known to be 0.066667 V per day (Rad-Elec, 2024). This is the voltage reduction expected for a charged electret in the absence of ionizing radiation. The standard calculation algorithm for RnC corrects for the predicted IVD. For the Figure (2) experiment, the expected IVD for the duration would be 0.2 volts, which is not greatly different than the measured blank,

but obviously much less than that seen with the cave sensors. Clearly, something more than IVD was happening in the Figure (2) trials.

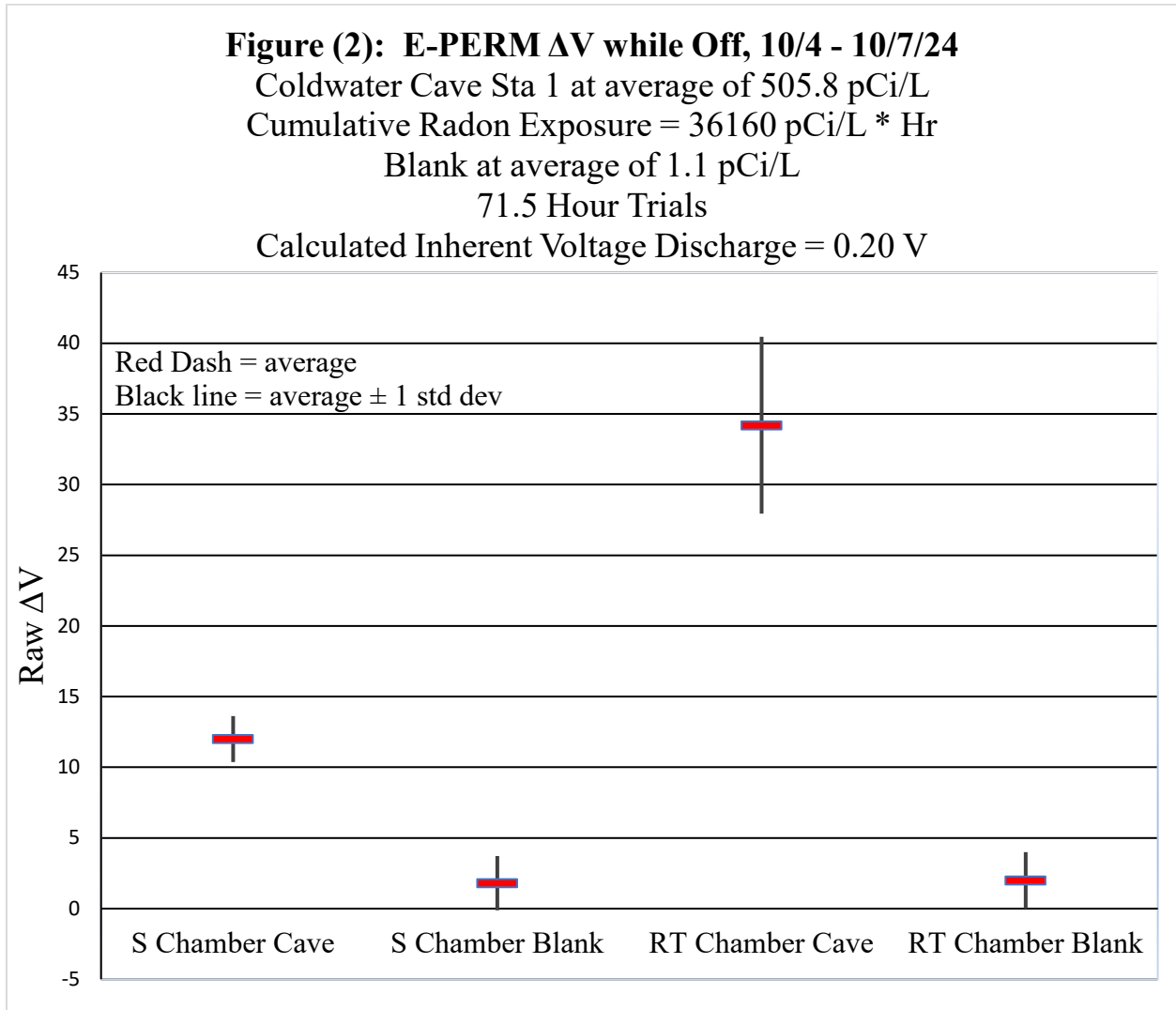


Figure (2): E-PERM ΔV while in the Off Position, 10/4-10/7/24, Coldwater Cave Sta. 1, using ST electrets.

Examining (see Figure (3)) the construction of the E-PERM, the diameter of the circular active electret surface was 1-1/4 inches, and when the plunger was down (when in the “off” position) it sat on the thermoplastic flange surrounding the electret surface, leaving a gap of about 1/16 of an inch between plunger and electret. The gap was important to avoid contact between the plunger and the electret surface when the sensor was jarred, as this would lead to voltage changes and erroneous data. However, this spacing leaves a small cylindrical volume between the plunger and the electret with a volume of 0.77 cubic inches (1.3 ml) which could serve as an active chamber for electret functioning. The plunger sitting atop the electret flange served as a barrier that would slow gas access to the active chamber, but not prevent it for a small specie such as a radon atom. As for the mechanism for radon to reach this active chamber while the sensor was

in the off position, the majority of the thermoplastic S chamber would look to be impermeable to gases like radon. This left radon to diffuse through the gap between the cap and the body of the chamber (entry point A in Figure (4)) and further downstream having to pass through the filter in the neck of the chamber, and/or radon passing through the space between where the electret was threaded into the chamber body (entry point B in Figure (4)). Neither was wide open by any means, but on the other hand they did not look to be sealed and radon has a small cross-section given that it is in the atomic form. The difference in signal for the in-cave sensors between the S and the RT chambers was illuminating. Since RT chambers are constructed from an S chamber, the geometric factors should produce active chambers of exactly the same size. However, in addition to entry points A and B for the S chambers, the Tyvek-covered pores that have been drilled into the thermoplastic walls of the RT chamber provide an additional rapid pathway for radon to enter the chamber (entry point C in Figure (4)). This explains the higher ΔV signal seen in Figure (2) for the RT cave sensors as compared to the S chambers. Both have active chambers of equal size and sensitivity, but the radon enters the RT chamber much more quickly, and this will lead to larger displayed ΔV values when the time for radon to enter the active chamber is a limiting factor.

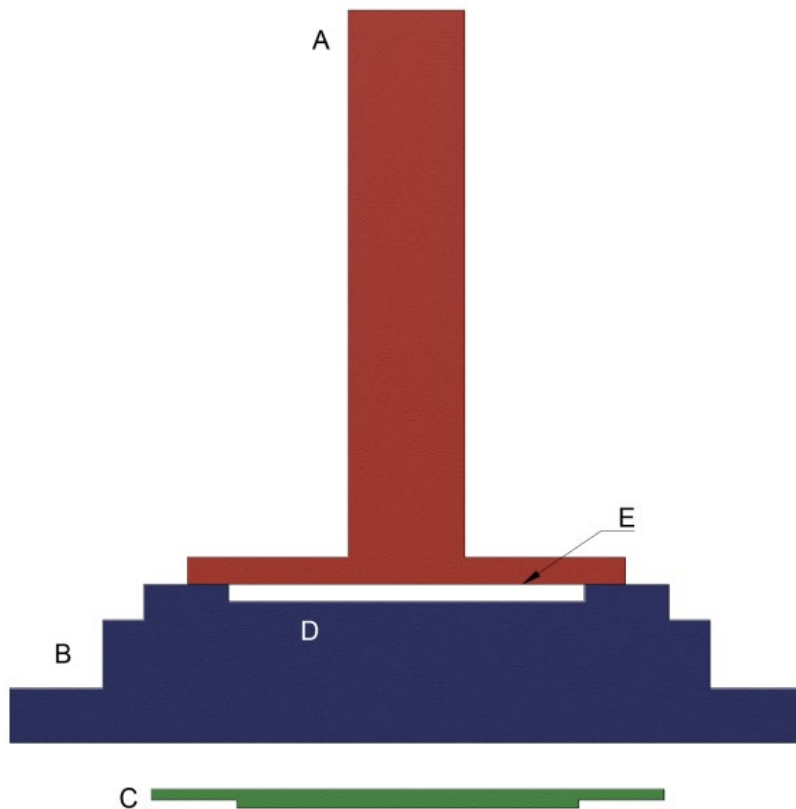


Figure (3): Scale cross-sectional profile diagram of the plunger – electret interface for an E-PERM in the off position. A (in red) is the plunger. B (in blue) is the electret. C (in green) is the PETG spacer. D is the position of the positively-charged electret surface. E is the active chamber. For scale reference, the plunger bottom width is 1.6 inches.



Figure (4): Potential entry points for radon with the chamber in the Off Position. E-PERM S chamber on the left, RT chamber on the right. A is under the cap, B is through the threads where the electret is screwed in, C is through the Tyvek-covered pores on the body of the RT chamber.

Given that the chambers were never opened during the trials as would happen during normal E-PERM operation, the algorithm to calculate radon concentration was not valid, and the experimental output was left in units of ΔV . However, since it was known that E-PERM sensitivity is a function of the electret voltage, prior work using ΔV units used algorithms to normalize the impact of the electret voltage (Welch, 2023, 2024). This normalization depends on calculating a calibration factor (CF) for the specific electret utilizing its specific midpoint voltage (MPV, the average of the initial and final voltages) as seen in Equation (2).

The A and B coefficients are constants for a particular chamber type and electret type. These values are known for S chambers combined with ST electrets, but the coefficients are only valid for the geometry of the chamber when it is in the on position. Given that this experiment utilized the off position, the standard A and B coefficients should not be used to calculate CF values, thus the experimental output could not be normalized, and was left in units of ΔV .

The electret voltages for the sensors used to produce Figure (2) had not been considered, and the replicate sets contained a fair bit of variance in MPV. To ensure that this was not impacting the outcome of the trial, the Figure (2) experiment was repeated with an effort made to start the trials with electrets with as similar an initial voltage as possible, thus ensuring similarity in MPV values and therefore, CF values. Complete control of the MPV was not possible, given the finite number of electrets available and an inherent inability to control final voltage values. Sensor sets were put together to minimize the spread of initial voltages within a set and to keep the set

averages as close together as possible. The outcome of this experiment is shown in Figure (5), with the details of the electret MPV values summarized in Table 1.

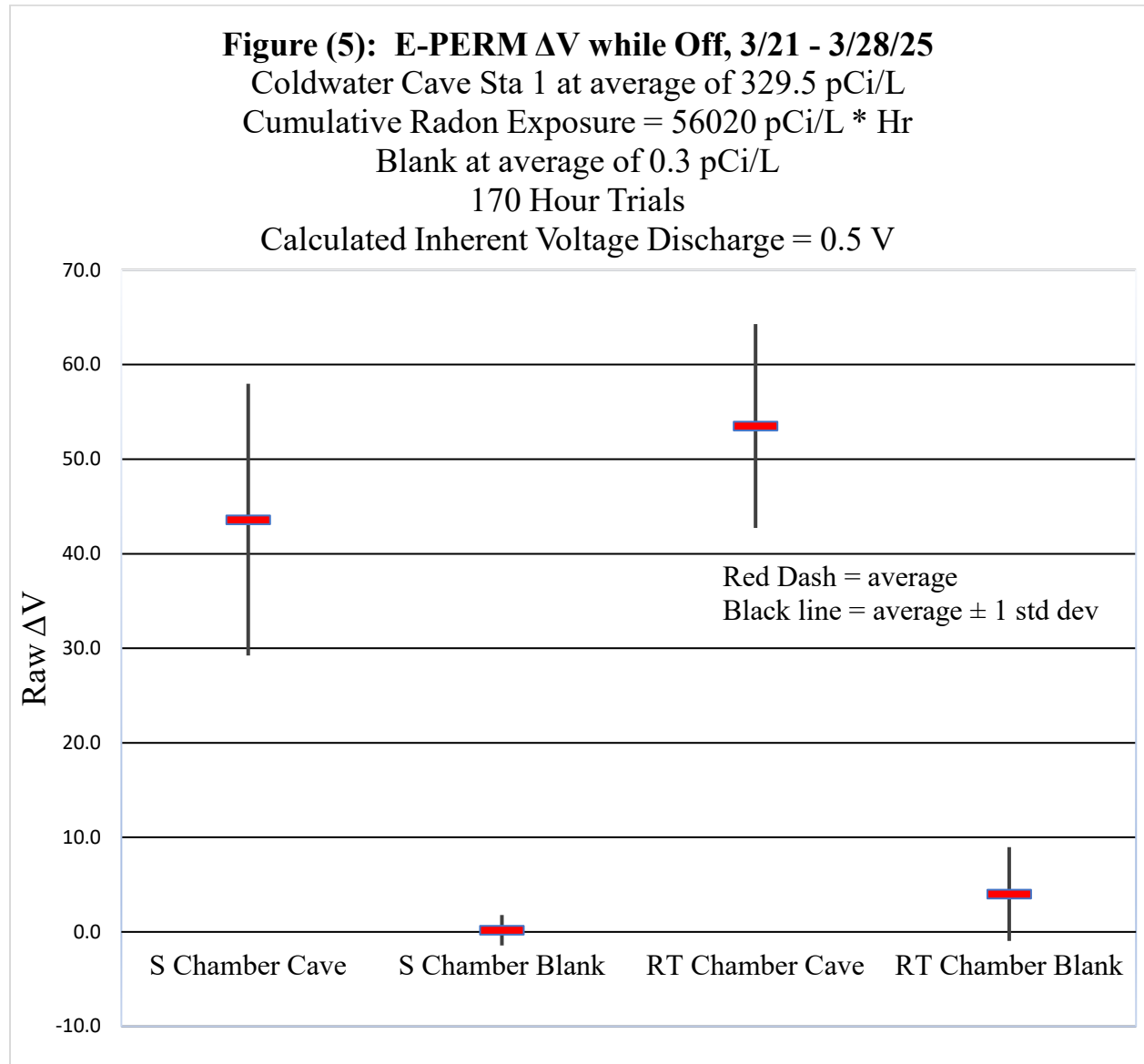


Figure (5): E-PERM ΔV while in the Off Position, 3/21-3/28/25, Coldwater Cave Sta. 1, using ST electrets.

The Figure (5) findings corroborate the significant differences between cave and blank sets seen in Figure (2) while clarifying that varying electret MPVs were not producing these differences. One interesting outcome of the Figure (5) trials was that although the cave RT chamber set still produced a higher average ΔV than the cave S chamber set, the proportion of the gap was smaller in relative terms. This is likely due to having a much longer experimental duration. Since the S chamber lacks the Tyvek-covered side ports into the chamber, radon ingress into the

chamber is slower than for the RT chamber. For a short experimental duration the ingress rate has a large impact on the measured ΔV , but a longer experimental duration like that for the Figure (5) trials will tend to reduce the impact of the slower radon entry on the ΔV . Similar efforts were made to reduce the differences in initial electret voltages for the balance of the trials in this study.

Table 1: Midpoint Voltage Set Averages and Standard Deviations for the Figure (5) Experiment.

Sensor Set	Avg. MPV	Std. Dev.
S Chamber Cave	618.4	13.1
S Chamber Blank	642.8	8.9
RT Chamber Cave	646.3	6.4
RT Chamber Blank	673.8	6.9

It was deemed important to rule out that the difference in ΔV could be attributed to external radiation sources in the cave that would not be present in the blank environs. This was considered not likely to be a factor based on prior work (Welch, 2022), but was tested anyway. This involved running a set of six E-PERMS in the off position at Coldwater Cave Station 1 while surrounded by lead plating, and simultaneously running a control set nearby with no lead shielding. The specifics of the lead plating enclosure are described in the Materials and Methods section. Each of the electrets were installed in their respective chambers with a torque of 1.0 ft-lb using the ETD (described in the Materials and Methods section), to pursue consistency in the permeability of the chambers held in the off position to environmental radon.

Table 2 summarizes the two trials undertaken comparing lead shielding with no lead shielding. Neither trial features a statistically significant difference between the two conditions, suggesting that background radiation was not a factor in the differences in ΔV observed in Figures (2) and (5).

Table 2: Comparing E-PERM sets with and without Lead Shielding while in the Off Position, Coldwater Cave Sta. 1, S chambers, electrets tightened to 1.0 ft-lb.

Set	Avg MPV	SD MPV	CRE	Avg ΔV	SD ΔV
6/9 - 6/13/25 With Pb Shielding	637.8	32.5	51870	17.5	3.4
6/9 - 6/13/25 Without Pb Shielding	618.9	33.8	51870	20.2	2.0
6/21 - 6/27/25 With Pb Shielding	596.9	35.0	49300	20.2	1.7
6/21 - 6/27/25 Without Pb Shielding	618.8	31.7	49300	19.5	4.1

Given the absence of significant contribution from external radiation to the observed ΔV , the hypotheses that the off position active chamber still had enough volume to reduce the electret voltage when radon was present, and that radon was able to reach this active chamber, appeared to be more robust. Further experimentation to probe these hypotheses was undertaken. The S chamber appeared to hinder entry of radon into the closed chamber significantly more than the RT chamber. Trials were designed to add further barriers to radon ingress, with expectation that this would significantly reduce the measured ΔV for the electrets. E-PERMs in the off position were sealed in a nested set of Ziploc® seal top polyethylene bags, placed at Station 1 in Coldwater Cave, and compared to a control set where the polyethylene bags were not used. In one of the trials, the E-PERM was encapsulated in not only a set of the polyethylene bags, but also installed within a sealed watertight Daren Drum for additional hindrance to radon entry. In all trials, the electrets were tightened to 1.0 ft-lb of torque. The results of these trials are summarized in Table 3. Clearly, radon can penetrate the sealed bags, but at a hindered rate resulting in a lower ΔV . The sets with 4X nested bags gave very consistent attenuation compared to the control signal, and as expected, the set with 8X nested bags inside a sealed Daren Drum yielded very little signal at all. Not only do these data confirm that hindering the ingress of radon will reduce the observed ΔV signal, but they also support the prior conclusion that background ionizing radiation was not a significant factor, as the thin polyethylene barriers would provide minimal shielding from external gamma and beta radiation yet were able to reduce the ΔV signal considerably.

Table 3: Comparing E-PERM sets with and without polyethylene barriers, Coldwater Cave Sta. 1, S chambers, ST electrets, electrets tightened to 1.0 ft-lb.

Set	Avg MPV	SD MPV	CRE	Avg ΔV	SD ΔV	% of Control
6/15 - 6/20/25 E-PERMs in 4X nested Ziploc	573.4	24.3	64330	12.0	3.5	58.3
6/15 - 6/20/25 Control	591.3	35.1	64330	20.6	4.2	
6/27 - 7/5/25 E-PERMs in 4X nested Ziploc	553.1	37.7	113180	20.6	3.3	57.4
6/27 - 7/5/25 Control	563.3	38.8	113180	35.9	7.1	
7/5 - 7/9/25 E-PERMS in 8X nested Ziploc + Daren Drum	591.1	37.1	62770	2.6	1.1	12.6
7/5 - 7/9/25 Control	598.2	31.8	62770	20.7	4.0	

Another type of experiment was used to probe the notion that the S and RT chambers in the off position had enough volume between the plunger and the electret surface to serve as active chambers for normal EIC function. The idea was to insert a plastic spacer into this active chamber to reduce its volume, which should attenuate the ΔV signal if the active chamber was functioning as an EIC. Less volume equates to both less radon in the chamber plus a lower probability of ionizing radiation from a radioactive decay striking a proximate air molecule and producing an electron. Each of these would mean fewer electrons collected by the electret surface. Although the active chamber had a measured thickness of 1/16 inch, filling too much of this space was perceived as a risk to data quality, as this increased the chances of voltage

Table 4: Spacer vs No Spacer for S and RT chamber E-PERMs in Off Position, Coldwater Cave Sta. 1, ST electrets, electrets tightened to 1.0 ft-lb.

Set	Avg MPV	SD MPV	CRE	Avg ΔV	SD ΔV	RSD (%) ΔV	Stat Sig Diff?
7/9 – 7/13/25 S chamber control, no Spacer	537.1	41.6	61220	16.4	3.5	21.4	No
7/9 - 7/13/25 S chamber with Spacer	523.4	37.1	61220	15.7	14.9	95.0	No
7/9 – 7/13/25 RT chamber control, no Spacer	498.8	23.8	61220	38.2	9.7	25.4	Yes
7/9 - 7/13/25 RT chamber with Spacer	487.5	42.3	61220	22.2	7.2	32.5	Yes
8/22 – 8/26/25 S chamber control, no Spacer	515.1	42.6	83950	20.7	2.9	14.1	Yes
8/22 - 8/26/25 S chamber with Spacer	504.5	44.8	83950	7.9	4.7	59.4	Yes
8/22 – 8/26/25 RT chamber control, no Spacer	458.8	25.9	83950	38.8	5.0	12.9	No
8/22 - 8/26/25 RT chamber with Spacer	456.4	43.5	83950	28.8	22.1	76.8	No

excursions from a spacer contacting the active surface of the electret, especially given the jostling expected in the handling and transport of the sensors. The best design led to circular spacer that fit over the top of the flange surrounding the electret surface, and then extending downward to fill a portion of the active chamber space. See Figure (3) for a scale depiction of the spacer, which is described in the Materials and Methods section. When in use for an off-position trial it would fit between the plunger and the installed electret.

Table 5: Detailed Look at Raw Data from 7/9 – 7/13/25 Sets using S chambers With and Without Spacers.

	7/9 – 7/13/25 S chamber control, no Spacer	7/9 - 7/13/25 S chamber with Spacer	7/9 - 7/13/25 S chamber with Spacer, after Grubbs Test
Sensor 1 ΔV	15	3	3
Sensor 2 ΔV	13	36	36
Sensor 3 ΔV	17	38	38
Sensor 4 ΔV	15	3	3
Sensor 5 ΔV	17	10	10
Sensor 6 ΔV	23	8	8
Sensor 7 ΔV	12	76	
Sensor 8 ΔV	19	12	12
Set Avg	16.4	23.3	15.7
Set SD	3.5	25.4	14.9

Two trials with and without spacers were run for both the S chamber E-PERMS and the RT chamber E-PERMS with the chamber in the off position, with the data summarized in Table 4. One of the S chamber sets showed a statistically significant reduction in electret ΔV , one did not. One of the RT chamber sets showed a statistically significant reduction in electret ΔV , one did not. All sets had in common that the spacer trials had decreased precision, as each had a relative standard deviation much greater than the no-spacer counterpart. To help illustrate what was happening, a detailed look at the data from one of the sets not showing a significant difference is displayed in Table 5. The spacer trials had a number of data points that showed the expected reduction in ΔV due to the smaller active chamber, but that was coupled with a handful of other points with much larger ΔV values than those seen in the no spacer trials. These were likely sensors where the spacer had made physical contact with the electret surface, causing a jump in voltage. Deploying the sensors in a cave involved significant transport issues, and some jostling of the sensors was inevitable, making spacer-electret contact more likely. Given the large relative uncertainty produced by having a set with some low values and some high values, it was difficult to confirm a statistically significant drop in voltage for the set overall. The

increased relative standard deviation for the spacer trials underlines the risk of reducing the standard 1/16-inch gap between the S chamber plunger and the electret surface when the chamber is in the off position. The chamber design maintaining this gap in retrospect looks like a wise choice.

As noted before, attempts to normalize the ΔV output units being reported were thwarted by the inability to calculate Calibration Factors (CF), as the necessary A and B coefficients for use in Equation (2) were only known for the chambers when they were used in the on position. An experiment was designed to determine the A and B coefficients for the chambers when in the off position. If the sensitivity of the sensor increased systematically with electret voltage, this would serve as a confirmation that the small active chamber created in the off position was of large enough volume for the sensor to behave as expected for a true EIC sensor, and it could permit normalization of raw ΔV readings for future experiments.

The theory behind the experimental setup is reviewed in the Materials and Methods section. Three replicate trials using 12 RT chambers in the off position were undertaken, with the resulting plots given in Figure (6) and the calculated A and B coefficients shown in Table 6.

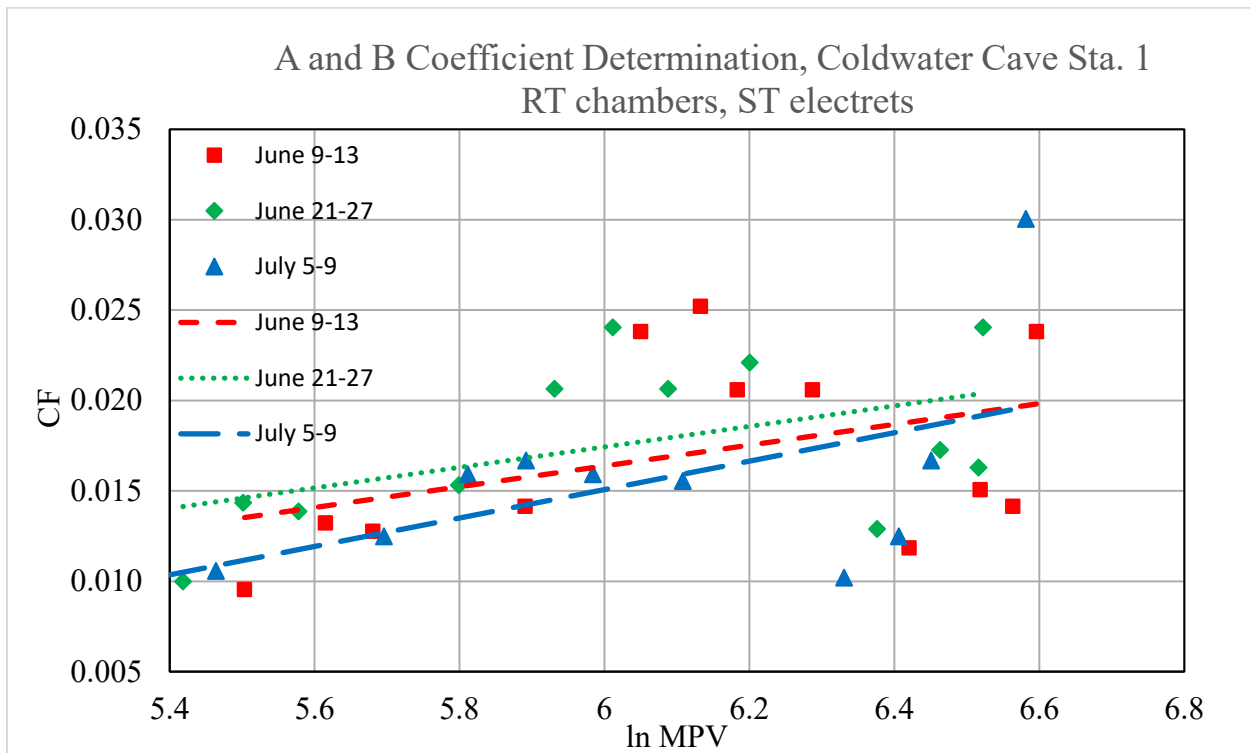


Figure (6): Three trials of the A and B coefficient determination experiment with raw data points and line fits given, Coldwater Cave Sta. 1, RT Chambers, ST electrets.

Table 6: A and B Coefficient Data Extracted from the Figure (6) Trials

Set	A	B	R ²	CRE
June 9-13, 2025	-0.0181	0.00575	0.1638	51870
June 21-27, 2025	-0.0166	0.00567	0.2397	49300
July 5-9, 2025	-0.0321	0.00786	0.3725	62770
3-trial Composite	-0.0244	0.00677	0.2667	54650

For comparison, the values provided by the vendor for the S and RT chambers, paired with ST electrets and in the on position, are 0.314473 for A and .260619 for B (Rad-Elec, 2024). Given Equation (2), the B coefficient serves as a sensitivity term, and it can be seen that the sensor in the off position was considerably less sensitive than when it was on, which made sense. Obviously, the precision of the experimental data was poor, which should be expected given the low signal-to-noise ratio that was produced by running a sensor in its off position. However, the calculated line fits and coefficients were remarkably reproducible, given the uncertainty. The plots also illustrate that there was a clear increase in CF as the midpoint voltage was increased, which was what would be expected for a functioning EIC sensor. So even in the off position, the E-PERM continues to produce a ΔV signal for environmental radon, just with much less sensitivity than when the unit was in the on position due to the much smaller size of active chamber and greatly hindered ingress of radon when the unit was closed.

Conclusions

E-PERMs still served as functioning EIC sensors when the electret was installed yet the chamber kept in the off position. As expected, the sensitivity, signal-to-noise, and precision were much smaller when the chamber was on. This means that radon gas was able to access the active chamber of the sensor when it was in the off position, and that, while small, the active chamber was voluminous enough to allow standard EIC behavior that produces reduction in electret voltage in the presence of radon. Probing studies with polyethylene barriers found that when the radon ingress pathway was hindered further, that the recorded electret ΔV was further reduced. Trials to determine A and B coefficients for the S and RT chambers in the off position were noisy yet successful, and they illuminated that the E-PERMs had an increased sensitivity to radon as the MPV of the electret was increased, which was consistent with predicted EIC behavior.

From a practical perspective, E-PERM ΔV changes while in the off position were only noticeable when the CRE value was very large for the duration. As long as an operator avoids lengthy storage of installed electrets or avoids zones with excessively high radon, there should be

no concerns with off-position ΔV alteration impacting experimental data. Redesigning the E-PERM chamber to reduce the plunger-electret span and therefore reduce the sensitivity of the sensor in the off position would not be recommended, as spacer studies underlined that reduction of this span led to an increase in data uncertainty and a degradation of sensor performance, likely due to the spacers contacting the electret.

Acknowledgements

This study would not have been possible without the generous access privileges granted by the landowner of the study cave. Knox College provided financial support to enable this research. The authors would like to thank the Knox College MakerSpace Network for the use of their design and fabrication resources, and Alex Fluegel for his assistance with mechanical drawings. Experimental and theoretical assistance was provided by Beth Welch and Chuck Schulz. Special thanks for all their assistance to the folks at Rad Elec.

References

- Fjeld, R.A., Montague, K.J., Haapala, M.H., and Kotrappa, P., 1994. Field Test of Electret Ion Chambers for Environmental Monitoring. *Health Physics*, 66(2), pp. 147-154.
- Grubbs, F., 1969. Procedures for Detecting Outlying Observations in Samples. *Technometrics* 11(1), pp. 1-21.
- Harris, D.C., 2017. *Quantitative Chemical Analysis*, 9th Ed. W.H. Freeman, New York.
- Kotrappa, P., Dempsey, J.C., Hickey, J.R., and Stieff, L.R., 1988. An Electret Passive Environmental ²²²Rn Monitor Based on Ionization Measurement. *Health Physics*, 54(1), pp. 47-56.
- Kotrappa, P., Dempsey, J.C., Ramsey, R.W., and Stieff, L.R., 1990. A Practical E-PERMTM (Electret Passive Environmental Radon Monitor) System for Indoor ²²²Rn Measurement. *Health Physics*, 58(4), pp. 461-467.
- Kotrappa, P. and Steck, D., 2010. Electret Ion Chamber-Based Passive Radon-Thoron Discriminative Monitors. *Radiation Protection Dosimetry*, 141 (4), pp. 386-389.
- Kotrappa, P., Stieff, L., and Stieff, F., 2014. Attenuation of Thoron (²²⁰Rn) in Tyvek Membranes. *Proceedings of the 2014 International Radon Symposium*, pp. 1-9. https://aarst.org/proceedings/2014/12_Kotrappa_ATTENUATION_OF_THORON_Rn220_IN_TYVEK_MEMBRANES.pdf.
- Rad-Elec, 2024. *E-PERM® System User's Manual*, Version 4.0.1.
- Rumble, J.R., Editor-in-Chief, 2018. *CRC Handbook of Chemistry and Physics*, 99th edition. CRC Press, Boca Raton, Section 11.
- Stacks, A.M. ed., 2015. *Radon: Geology, Environmental Impact and Toxicity Concerns*. Nova Science Pub., Hauppauge, NY, pp. 1-42.
- Stieff, A., Kotrappa, P., and Stieff, F., 2012. The Use of Barrier Bags with Radon Detectors. *Proceedings of the 2012 International Radon Symposium*, pp. 67-79. http://aarst-nrpp.com/proceedings/2012/04_THE_USE_OF_BARRIER_BAGS_WITH_RADON_DETECTORS.pdf.
- Welch, L.E., Paul, B.E., and Jones, M.D., 2016. Use of Electret Ionization Chambers to Measure Radon in Caves. *Proceedings of the 2016 International Radon Symposium*, pp. 1-18. http://aarst-nrpp.com/proceedings/2016/Welch_USE_OF_ELECTRET_IONIZATION_CHAMBERS_TO_MEASURE_RADON_IN_CAVES.pdf.
- Welch, L.E., Paul, B.E., Miller, E.C., Chen, Y.I., Jones, M.D., and Beck, C.L., 2017. Depth Profiling of Radon in Vertical Shafts Using Electret Ionization Chambers. *Proceedings of the 2017 International Radon Symposium*, pp. 1-18. <http://aarst-nrpp.com/proceedings/2017/DEPTH-PROFILING-OF-RADON-IN-VERTICAL-SHAFTS-USING-ELECTRET-IONIZATION-CHAMBERS-WELCH.pdf>.

Welch, L.E., Chen, Y.I., Jones, M.D., and Beck, C.L., 2019. Correlating Radon Activity with Carbon Dioxide Concentration in an Iowa Cave. Proceedings of the 2019 International Radon Symposium, pp. 11-25. <https://aarst.org/proceedings/2019/CORRELATING-RADON-ACTIVITY-WITH-CARBON-DIOXIDE-CONCENTRATION-IN-IOWA-CAVE-WELCH-2019.pdf>.

Welch, L.E., Paul, B.E., Takashima, A., Rau, G.D., Beck, C.L., Klausner, E.C., Miller, E.R., Jones, M.D., and Lace, M.J., 2021. Contextualizing Radon Activity in Northeastern Iowa Caves by Measuring Uranium and Thorium at the Radon Sampling Sites. Proceedings of the 2021 International Radon Symposium, pp. 1-14. https://aarst.org/proceedings/2021/Welch_Contextualizing-Radon-Activity-in-Northeastern-Iowa-Caves-2021.pdf.

Welch, L.E., Art, E.J., Rau, G.D., Beck, C.L., Frana, M.J., Klausner, E.C., Miller, E.R., Jones, M.D., and Lace, M.J., 2022. Evaluating the E-PERM RT Chamber for use Measuring Rn-220 in a Cave Environment. Proceedings of the 2022 Indoor Environments (AARST) – Radon and Vapor Intrusion Symposium pp. 1-17. https://aarst.org/proceedings/2022/Welch_EVALUATING_THE_E-PERM_RT_CHAMBER_FOR_USE_MEASURING_RN-220_IN_A_CAVE_ENVIRONMENT.pdf.

Welch, L.E., Doughty, R.M., Art, E.J., Beck, C.L., Jones, M.D., and Lace, M.J., 2023. Evaluating the Electret Radon Progeny Integrated Sampling Unit for use Measuring Radon and Radon Progeny in a Cave Environment. Awaiting publication in the Proceedings of the 2023 Indoor Environments – Radon and Vapor Intrusion Symposium.

Welch, L.E., Paschke, K.A., Doughty, R.M., Klausner, E.C., Jones, M.D., and Lace, M.J., 2024. Characterizing Post-Trial Carryover of Signal When Using E-PERM and Electret Radon Progeny Integrated Sampling Unit Sensors in a High Radon Cave Environment. Awaiting publication in the Proceedings of the 2024 Indoor Environments – Radon and Vapor Intrusion Symposium.